Morphological and genetic differentiation of *Bufo* toads: two cryptic species in Western Europe (Anura, Bufonidae)

Jan W. Arntzen[1], Jacob McAtear[1], Ernesto Recuero[2,3], Janine M. Ziermann[1,4], Annemarie Ohler[5], Jacques van Alphen[1], Iñigo Martínez-Solano[6,7,8]

[1] *Naturalis Biodiversity Center, P.O. Box 9517, 2300 RA Leiden, The Netherlands*
[2] *Museo Nacional de Ciencias Naturales, CSIC, c/ José Gutiérrez Abascal, 2, 28006 Madrid, Spain*
[3] *present address: Departamento de Ecología de la Biodiversidad, Instituto de Ecología, Universidad Nacional Autónoma de México, Ap. Postal 70-275, Ciudad Universitaria, México DF, 04510, Mexico*
[4] *present address: Dept. of Anatomy, Howard University, College of Medicine, 520 W St. NW, Washington DC 20059, USA*
[5] *Muséum national d'Histoire naturelle, Département Evolution et Systématique, UMR 7205 CNRS Origine, Structure et Évolution de la Biodiversité, 25 rue Cuvier, CP 30, 75005 Paris, France*
[6] *Instituto de Investigación en Recursos Cinegéticos (IREC), CSIC-UCLM-JCCM Ronda de Toledo, s/n 13071 Ciudad Real, Spain*
[7] *present address: CIBIO (Centro de Investigação em Biodiversidade e Recursos Genéticos), Rua Padre Armando Quintas, s/n, 4485-661 Vairão, Portugal*
[8] *E-mail: inigomsolano@gmail.com*

Abstract

The Common toad *Bufo bufo sensu lato* is a widespread, morphologically conserved taxon. Recent studies have uncovered deep genetic differentiation between population groups, highlighting the need to revise the current taxonomy of the group and recognize additional species. Here we investigate patterns of variation in molecular (a mitochondrial DNA restriction enzyme assay and sequence data for two nuclear DNA fragments totalling 979 bp) and 17 morphological variables in Northern France where two of these groups meet (*B. bufo sensu stricto* and *B. spinosus*), in order to delineate their contact zone and uncover characters that would allow discrimination of the two taxa. Mitochondrial DNA data show an abrupt transition from areas where *B. bufo* is present to those inhabited by *B. spinosus*, with a narrow area of overlap east of the city of Caen. Morphometric characters, particularly those related to the positioning of the parotoid glands and metatarsal tubercle shape and size, proved useful in discriminating between species (AUC ≥ 0.97, kappa ≥ 0.79). We then used the differentiating character states to allocate over 300 museum specimens from Western Europe to either species with consistent results, including comparable values of AUC and kappa of the identification models, indicating that models could successfully be applied across datasets. We summarize available evidence relevant to the delineation of the distribution of *B. bufo* and *B. spinosus* in France and discuss the characters differentiating both species in an evolutionary context. In view of

the observed morphological and genetic differentiation and the absence of unequivocal evidence for widespread hybridization we support the view that *B. bufo* and *B. spinosus* are best considered different species. Finally, we propose that 'parotoids in parallel position' and a thin and smooth skin are derived character states for *B. bufo* over the northern part of its range.

Contents

Introduction

The range of the Common toad *Bufo bufo* (Linnaeus, 1758) *sensu lato* stretches from Morocco in the southwest to near Lake Bajkal, Russia, in the east. In Scandinavia it is found north of the Arctic Circle. It is absent from all major Mediterranean islands except Sicily and there are also populations in the British islands, although it is not present in Ireland. Closely related Eurasian species are *B. eichwaldi* Litvinchuk, Borkin, Skorinov and Rosanov, 2008 and *B. verrucosissimus* (Pallas, 1814) in the Caucasus, with ranges adjacent to the Caspian Sea and the Black Sea, respectively. Recent work demonstrates the existence of two genetically differentiated, western and eastern groups within the Common toad. The western group conforms to *B. spinosus* Daudin, 1803 and is distributed in Northern Africa (from Morocco to Tunisia), Iberia and a large part of France. The eastern group conforms to *B. bufo* (Linnaeus, 1758) and is distributed from Northern and Eastern France to deep into Scandinavia and Russia. It occurs in the Northern Mediterranean region other than the Iberian Peninsula. The sister group of *B. bufo* is not *B. spinosus* but *B. verrucosissimus* (Recuero *et al.*, 2012). The molecular genetic differentiation between *B. bufo* and *B. spinosus* is deep, with a sequence divergence of 7.0% at mtDNA (uncorrected p-distance at the combined *16S* and *cytb* genes; Recuero *et al.*, 2012). With respect to nuclear DNA, allozymes show deep differentiation too (García Porta *et al.*, 2012, Arntzen *et al.*, 2013), whereas two out of the four nuclear genes studied by Recuero *et al.* (2012) are species diagnostic (the genes *BDNF* and *RPL3*). The latter study also found shared alleles in the genes *POMC* and *CXCR4*, although it is as yet unclear whether this results from limited introgression or incomplete lineage sorting (Arntzen *et al.*, 2013). The most recent ancestor of the *B. bufo* – *B. spinosus* – *B. verrucosissimus* group is estimated at 9.2 Ma (million years before present) (Recuero *et al.*, 2012). In spite of the deep and long-lasting species differentiation, the species are superficially similar, with no convincing information available on how they could be distinguished by morphology. While contact zones have been approximated based upon expert knowledge (Geniez and Cheylan, 2012: 132) and molecular data (Arntzen *et al.*, 2013), the precise range boundaries and potential extent of overlap between the species are yet to be documented.

We obtained new molecular and morphometric data in two fine-scale transects in Northern France. The aims of the study were to further delineate the contact zone of *Bufo bufo* and *Bufo spinosus* with mitochondrial and nuclear DNA markers and to uncover morphological character states that would allow the identification of adult *B. bufo* and *B. spinosus*. With selected characters we furthermore studied morphological variation in a transect across Western Europe using material from museum collections. On account of the observed morphological differentiation, the deep genetic differentiation, the absence of unequivocal signs of widespread hybridization or introgression of *B. bufo* and *B. spinosus* in the area we investigated and the sister-group relationship of *B. spinosus* and the *B. bufo* – *B. verrucosissimus* clade, we conclude that *B. bufo* and *B. spinosus* are best considered separate species.

Material and methods

Molecular identification and delineation of the contact zone

Species identity was determined by mitochondrial DNA restriction fragment length polymorphism (RFLP) analysis. A small tissue sample was taken from either adult toads or tadpoles by clipping off the tip of a toe or of tail, respectively, in five French populations that we knew (Recuero *et al.*, 2012) or anticipated to represent *Bufo bufo* (a - Audresselles, b - Autreppes and c - Sorques) and *B. spinosus* (d - Jublains and e - Gizeux) and in two latitudinal transects, with 12 localities from Audresselles to Jublains and 15 localities from Autreppes through Sorques to Gizeux (Fig. 1). The material was stored in 96% ethanol. Individuals were released at the place of capture. DNA was extracted with the DNeasy Blood and Tissue Kit (Qiagen). We PCR-amplified a fragment of the mitochondrial gene cytochrome-b (*cytb*), following the procedure described by Recuero *et al.* (2012). Documented *cytb* sequences were searched for the presence of restriction sites with CLC DNA Workbench (CLC Bio, Aarhus, Denmark). Considering expenditure and the size of the expected fragments in *Bufo bufo* and *B. spinosus* the restriction enzyme *Bcu*I was selected. The laboratory procedure followed the recommendations of the distributer (Fermentas, Germany). A mixture of 18 µl nuclease free water, 2 µl 10X Buffer Tango, 8 µl fresh PCR product and 1 µl restriction enzyme (10 u/µl) was incubated for two hours at 37°C. The reaction was stopped by adding 1 µl of 0.5M EDTA (pH 8) to the mixture. Subsequently, the products were loaded

on a 1% Agarose gel (5 μl product loaded; 1% Agarose in 0.5XTBE gel) for electrophoretic separation.

Additionally, to further delineate the contact zone and detect the possible presence of admixed populations, two nuclear DNA regions, *POMC* and *RPL3,* were amplified and sequenced in ten individuals from each of the five French populations included in the morphometric study (localities a through e, see Fig. 1). Laboratory protocols followed Recuero *et al*. (2012). Two haplotypes per individual were phased for each of the genes *POMC* and *RPL3* using SeqPHASE (Flot, 2010) and PHASE 2.1.1 (Stephens *et al*., 2001), under default settings. Haplotype networks were constructed with HaploViewer (available at http://www.cibiv.at/~greg/haploviewer) using a neighbor-joining tree reconstructed with PAUP* (Swofford, 2001). Sequences from *B. verrucosissimus, B. eichwaldi* and *B. gargarizans* Cantor, 1842 from Recuero *et al*. (2012) were used as outgroups.

Morphometrics

Seventeen morphological characters of toads from five French localities representing *Bufo bufo* (Audresselles, 11 males, 11 females; Autreppes, 15 males, 10 females; Sorques, 8 males, 3 females) and *B*. *spinosus* (Jublains, 13 males, 16 females; Gizeux, 11 males, 7 females) were measured in live toads that were within 18 hours released at the place of capture, from March 2 – April 4, 2012. Species affiliation was on the basis of the DNA profiles (as in results below). We measured snout-urostyle length (SUl), head width (Hw), parotoid length (Pl), parotoid width (Pw), forearm and hindlimb length (Fl, Hl), length of the first (innermost) and the third finger including the adjacent tubercle (F1l, F3l), length of the innermost and the fourth toe, including the adjacent tubercle (T1l, T4l), and length and width of the inner metatarsal tubercle (MTl and MTw, Fig. 2C). We also measured the anterior (Pda) and posterior parotoid distance (Pdp) to obtain 'parotoid divergence' (Pd=Pda/Pdp; Fig. 2A). Parotoids are frequently asymmetric or oddly shaped. Pl and Pw were therefore measured on both the left and the right side of the toad. The other characters were measured along the body axis [SUl and Pa (see below), Pda and Pdp] or on the right side of the body (the remaining characters). Measurements were taken with a ruler (SUl and Hl; with 0.5 mm precision), or callipers (with 0.1 mm precision; for the other characters). Sexes were easy to distinguish in the breeding season from the toad's behaviour and secondary sexual characteristics. Addi-

tionally, a photo was taken of the dorsal side of the head. A paper print was then used to measure the character 'parotoid angle' (Pa, Fig. 2B) with the help of a protractor (precision 0.5 degrees). We encountered some difficulties in measuring the relative position of the parotoids, as follows (see also Appendix V). The measurement Pd may be flawed when the position of the anterior or posterior end of the parotoid is unclear and when the parotoids are of unequal length. The measurement Pa is ambiguous when the parotoids are bean shaped or curved, because it is unclear where exactly to position the tangent (for examples see Muratet, 2008). Note that curved or 'oblique' parotoids such as depicted by Muratet (2008: 181, female) and Arnold *et al*. (1978: 72) were not encountered in the live material. A few were found in the museum material (n=11 in *B. bufo*, 12.2% and n=5 in *B. spinosus*, 2.3%) and in those cases Pa was measured over two stretches and the mean angle taken, according to the length of both stretches. The measuring of a subsample of 16 *B. spinosus* (eight males and eight females) was duplicated to assess inter-observer variation (V). V is defined as the average of $|(A_1-A_2)|/((A_1+A_2)/2)$, in which A is the character state as measured by observers 1 and 2. Directional asymmetry (DA) of the parotoids was measured the same way and fluctuating asymmetry (FA, small, random differences between sides of bilateral characters; index number 2 in Palmer and Strobeck, 1986) equals |DA|.

In a first, exploratory stage we performed discriminant analysis on the standardized residuals of the regression of ln-transformed morphometric data versus ln-transformed snout-urostyle length, with SPSS 21 (SPSS, 2013). The transformation was done in order to reduce the effect of variation in individual size and to increase the fit to the requirements for such analyses (Sokal and Rohlf, 1981). Four missing values (0.3% of the total data) were estimated with linear regression against SUl. The following, more focused analyses were with logistic regression for males and females separately. The fit of statistical models to the data was expressed with the area-under-the-curve statistic (AUC) and with Cohen's kappa (k, Cohen, 1960). To obtain criteria for species identification from untransformed data (that can be readily applied in the field) we described the size and the shape of the metatarsal tubercle (MTsize=MTl/SUl, MTshape= MTw/MTl) and the positioning of the parotoids (Pa and Pd).

The validity of the obtained criteria for morphological species identification was assessed through the
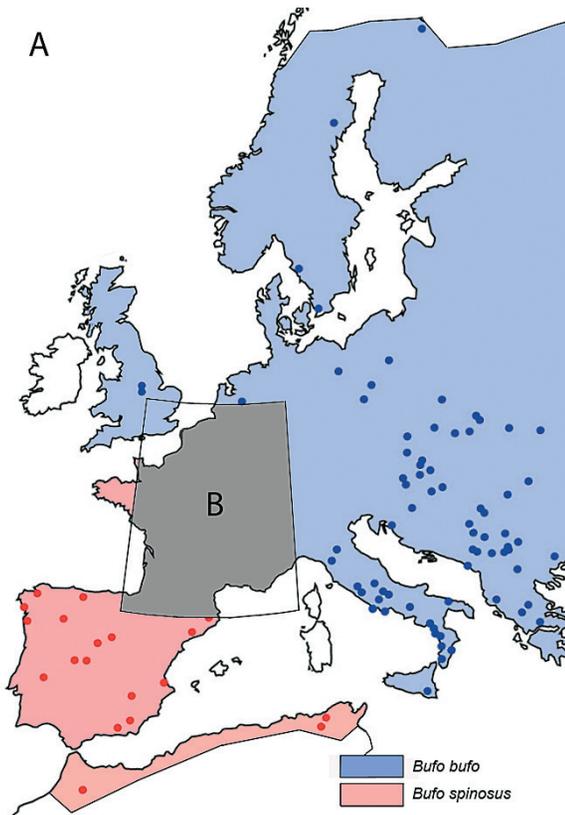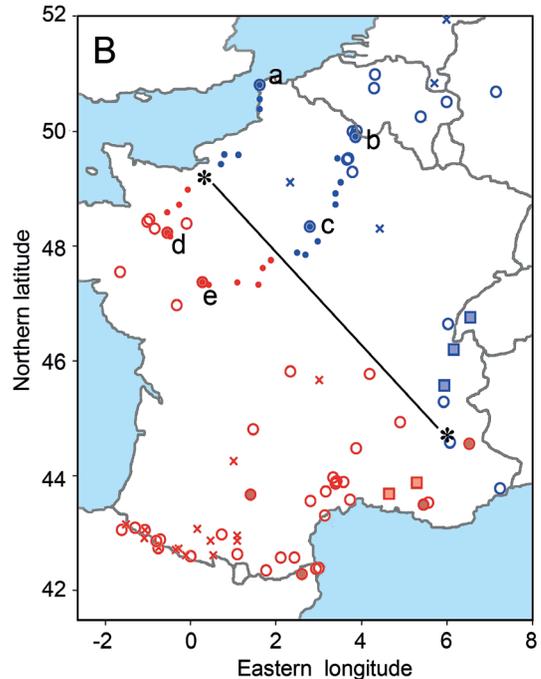
Fig. 1. A: Distribution of *Bufo* toads across Western and Central Europe. Populations identified with molecular data are shown by blue dots for *Bufo bufo* and by red dots for *B. spinosus,* from Recuero *et al.* (2012). The species' blanket distribution is shown with blue and red shades, after Sinsch *et al.* (2009). For a comprehensive overview of the available data see Appendix VIII.

B: Sampling localities for *Bufo* toads in France and adjacent areas. Populations subjected to morphological analyses are: a) Audresselles, b) Autreppes, c) Sorques, d) Jublains and e) Gizeux. Two transects studied for mtDNA RFLP fragments run from Audresselles to Jublains with 12 localities and from Autreppes, through Sorques to Gizeux with 15 localities (small round symbols). Two localities shown with an asterisk have mtDNA haplotypes for both species (Moyaux in Northwestern France, present paper, and Saint Bonnet en Champsaur in Southeastern France, Recuero *et al.*, 2012). Other populations with mtDNA identifications are shown by open round symbols (García-Porta *et al.*, 2012; Recuero *et al.*, 2012). Populations additionally identified with nDNA are shown by filled round symbols (Recuero *et al.*, 2012; present paper). Five populations identified with allozyme genetic data are shown by square symbols (data from Lüscher *et al.*, 2001) and localities with museum material are shown by crosses (see also Appendix I). Toads from localities northeast of the diagonal line are identified as *B. bufo* and those to the southwest of the line as *B. spinosus*.

analysis of preserved adult toads from 40 localities across Western Europe, as available at our home institutions, namely the Naturalis Biodiversity Center, Leiden (RMNH, n=67 in three populations), the Muséum national d'Histoire naturelle, Paris (MNHNP, n=43 in ten populations) and the Museo Nacional de Ciencias Naturales, Madrid (MNCN, n=196 in 27 populations) (Appendix I). Sex of the specimens was determined on secondary sexual characters or direct observation of the gonads. In addition to measuring the body size, parotoids and metatarsal tubercle we scored the spines on the cheek with the use of five classes (absent, light,

medium, strong and very strong, as in Appendix VII). However, scoring this character raised discussions among observers and we noted that the keratin spines may be related to reproductive state or sex of the specimens and also diminish with the shedding of the skin in preserved material and presumably in the field also. Finally, we measured Pa and Pd in 23 adult toads from published imagery (Muratet, 2008) and we reanalyzed data on the degree to which *Bufo bufo* and *B. spinosus* have smooth or spined warts, as originally recorded by De Lange (1973), using the same material that is deposited at the Leiden collection.
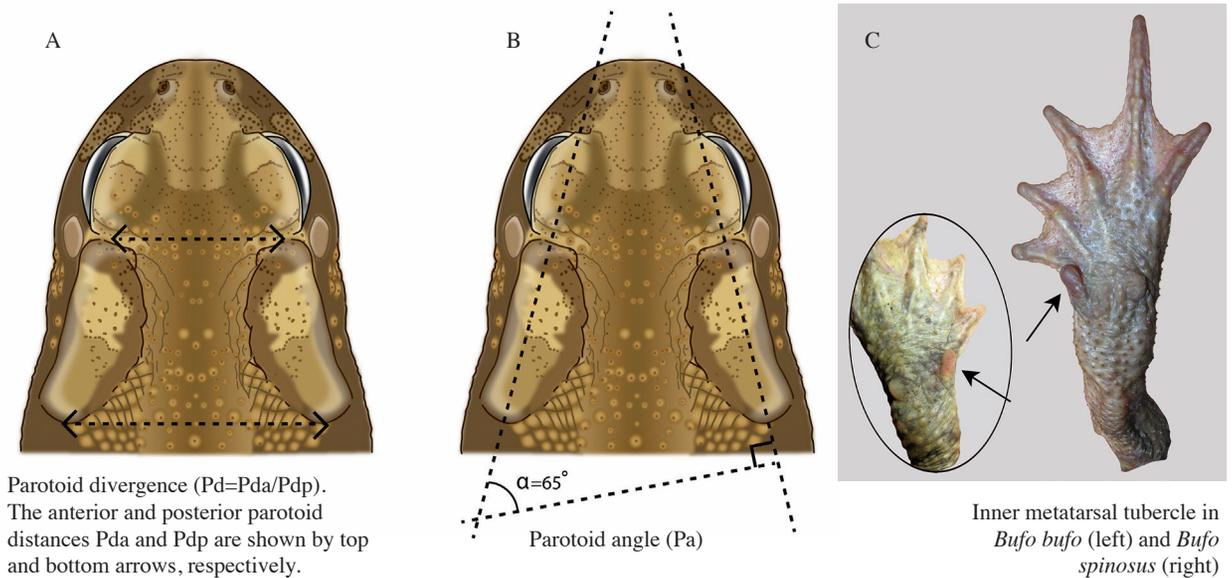
Parotoid divergence (Pd=Pda/Pdp). The anterior and posterior parotoid distances Pda and Pdp are shown by top and bottom arrows, respectively.

Parotoid angle (Pa)

α=65°

Inner metatarsal tubercle in *Bufo bufo* (left) and *Bufo spinosus* (right)

Fig. 2. Key characters in the morphological identification of *B. bufo* and *B. spinosus* toads. Parotoid positioning documented with parotoid divergence (Pd=Pda/Pdp, A) and parotoid angle (Pa, B). In this case, a parotoid angle of 65° would suggest this individual is a *B. spinosus*. C – inner metatarsal tubercle in *B. bufo* (left) and *B. spinosus* (right). Imagery from Muratet (2008) with permission. Unfortunately, the sex of both toads went unrecorded (J. Muratet, pers. comm.).

Results

Molecular identification and delineation of the contact zone

Different restriction profiles of *cytb* were obtained, one with two fragments of ca. 300 and 500 base pairs (bp) long and one with three fragments of ca. 100, 200 and 500 bp long (see Appendix II). The fragment sizes correspond to 86, 198 and 438 bp in *B. bufo* and 284 and 438 bp in *B. spinosus* in two randomly selected sequences for these species in GenBank. Out of 27 populations in the two transects studied (Fig. 1), 15 were equated with *B. bufo*, 11 were equated with *B. spinosus* and one population contained both types. This was locality 'Moyaux' (49.2 N, 0.3 E) where we found *B. bufo* type mtDNA six times and *B. spinosus* type mtDNA two times.

We obtained 50 new sequences of *POMC* (472 bp) and *RPL3* (507 bp) from ten individuals of each of the five French populations analyzed for morphometric characters (GenBank accession numbers KF745897-KF745924). These were analyzed alongside sequence data published by Recuero *et al*. (2012). In *POMC* we found 17 haplotypes, five of them exclusive of the outgroups (*Bufo gargarizans* and *B. eichwaldi*). Of the

remaining 12, two were shared between *B. bufo* and *B. verrucosissimus*, two were exclusive of *B. spinosus*, five were exclusive of *B. bufo* and the remaining three haplotypes were shared between *B. spinosus* and *B. bufo* in Audresselles (n=1), Autreppes (n=5) and Sorques (n=6), plus one toad from Erloy, close to Autreppes, reported by Arntzen *et al*. (2013) (see also Appendix VIII). In *RPL3* we found 57 haplotypes. Allele sharing across species was limited to *B. bufo* and *B. verrucosissimus* (one haplotype), with 15 haplotypes exclusive of *B. bufo*, 29 exclusive of *B. spinosus*, two exclusive of *B. verrucosissimus* and the remaining ten from the outgroups *B. eichwaldi* (seven haplotypes) and *B. gargarizans* (three haplotypes, Fig. 3).

Geographical distribution

The available data on the occurrence of *B. bufo* and *B. spinosus* in and around France are shown in Fig. 1. The mtDNA signature over two transects suggest that these species have parapatric ranges. A straight line can be drawn that approximates the mutual species border, from Caen at the Atlantic coast to Lyon in the upper Rhone valley, with *Bufo bufo* in the Northeast and *B. spinosus* in the Southwest of France. With respect to nuclear DNA data, *RPL3* is consistent with
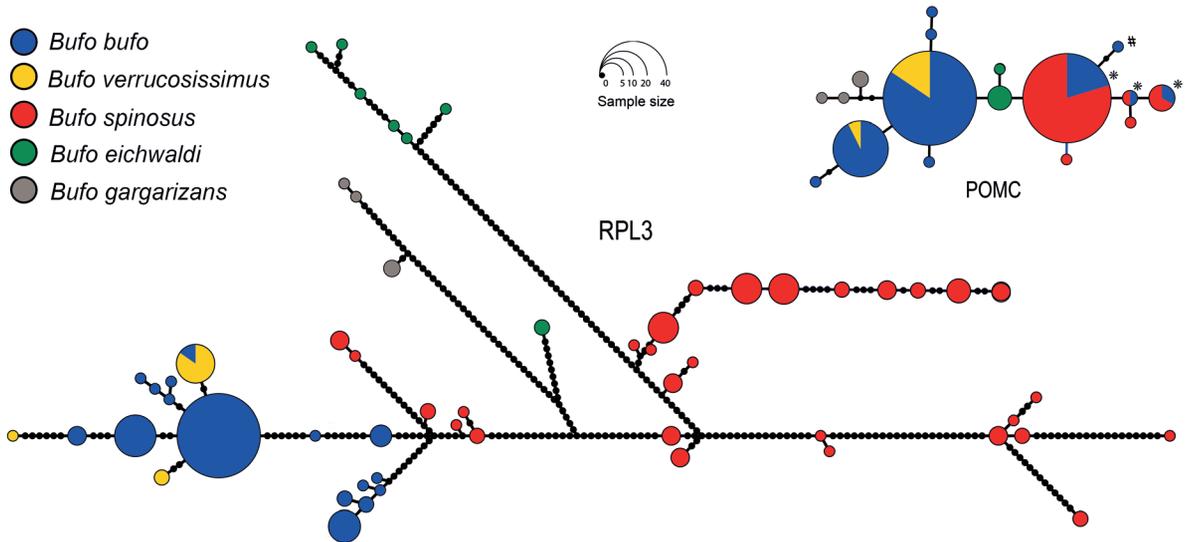
Fig. 3. Haplotype networks for *POMC* and *RPL3* in the *Bufo bufo* species group (colored by species, based on mtDNA profiles). Circles are proportional to sample size (see scale). Asterisks mark *POMC* haplotypes that are shared between *B. spinosus* and *B. bufo*. The symbol "#" highlights a "spinosus-like" allele that was found in an individual from the United Kingdom (BB04, see text).

mtDNA and morphometric data, whereas *POMC* alleles are shared across species in a wide area including the localities of Audresselles, Autreppes, Erloy and Sorques (*B. bufo*), and the French localities of Jublains, Gizeux, Beauzelle and La Manouesse, plus the Iberian populations of Capileira, A Pobra do Caramiñal, Portalegre, Laguna Grande de Gredos and Sadernes, and the north African localities Ifrane and Beni M'Tir (*B. spinosus*). Since nucleotide variation in *POMC* is low, with all haplotypes differing by a maximum of eight mutations, and because there is no clear geographic signal in the patterns of allele sharing, we conclude this most likely reflects incomplete lineage sorting rather than introgression or hybridization (as in marker *CXCR4* in Recuero *et al*., 2012, see Arntzen *et al*., 2013). For a comprehensive picture on the distribution of the four species in the *Bufo bufo* species group see Appendix VIII.

Morphological differentiation and identification

In discriminant analysis of both sexes of both species, the percentage of variance explained was 80.0% at the first axis and 15.8% at the second axis. The first axis had high loadings of the characters describing the positioning of the parotoids and the length and width of the metatarsal tubercle and proved useful for discrimination between the species (AUC = 0.94 ± 0.022,

kappa = 0.73). The second axis had high loadings of the characters describing leg- and toe-length and proved useful for discrimination of the sexes (AUC = 0.73 ± 0.050, kappa = 0.67). Inter-observer variation (V) was highest in the characters related to the metatarsal tubercle and the parotoids (5.2% < V < 8.6%), medium in the digit characters (3.6% < V < 6.2%) and low in the other characters (1.9% < V < 3.5%). Directional asymmetries at V and left-right differences in the parotoids (Pl and Pw) were insignificant. An analysis of variance with 'gender' nested under 'species' indicated that FA was higher in males than in females for Pl (P < 0.05) and marginally significant in Pw (0.05 < P < 0.10).

Logistic regression analyses with the characters SUl, Pa, Pd, MTsize and MTshape available for selection yielded well-fitting models for both sexes (AUC ≥ 0.97, kappa ≥ 0.79). The parotoid – and metatarsal tubercle measurements analyzed in isolation yielded lower, but by and large respectable model fit values (Table 1A; 'respectable scores' are here defined as AUC > 0.9 and kappa > 0.7). For the museum material the logistic regression analyses with the characters SUl, Pa, Pd, MTsize and MTshape available for selection also yielded well-fitting models for both sexes (AUC = 0.98, kappa ≥ 0.88). The parotoid and metatarsal tubercle measurements analyzed as separate sets yielded slightly lower model fit values with AUC

Table 1. Logistic regression models to distinguish (A) live *Bufo bufo* and *B. spinosus* in Northern France and (B) museum material of these species from across Western Europe. Either five variables were available for selection under a stepwise procedure (left panel) or variables were entered per character set (right panel). Note that under A body size (SUl) does not significantly contribute to species identification. Model fit is shown by AUC and kappa-values, in boldface type when values are respectable (AUC > 0.9, kappa > 0.7). N.s. = not selected. Example: the formula p=(1/(1+exp(-0.274*Pa-394.830*MTsize-31.596*MTshape+12.507))) calculates the probability (p) that a male toad is *B. bufo*.

A - Live toads in Northern France

| Morphometric variable | Full model | | Model per character set | | | |
| | | | Parotoids | | Metatarsus tubercle | |
	Males	Females	Males	Females	Males	Females
SUl	n.s.	n.s.				
Pa	-0.274	n.s.	-0.205	-0.113		
Pd	n.s.	-20.635	1.080	-10.968		
MTsize	394.830	288.545			142.592	273.790
MTshape	-31.596	n.s.			-21.609	-8.340
Constant	12.507	-0.973	13.513	16.530	3.268	-11.593
Model fit						
AUC	**0.98**	**0.97**	**0.91**	0.89	**0.93**	**0.91**
AUC standard error	0.012	0.024	0.046	0.049	0.031	0.045
Kappa	**0.86**	**0.79**	**0.76**	**0.70**	0.62	**0.75**
Model fit when applied to museum material						
AUC	**0.95**	**0.93**	0.89	**0.90**	0.89	0.85
AUC standard error	0.016	0.022	0.026	0.025	0.026	0.036
Kappa	**0.74**	0.61	0.52	0.62	0.55	0.52

B - Museum material from across Western Europe

| Morphometric variable | Full model | | Model per character set | | | |
| | | | Parotoids | | Metatarsus tubercle | |
	Males	Females	Males	Females	Males	Females
SUl	0.340	0.141	0.284	0.123	0.270	0.179
Pa	n.s.	-0.188	-0.084	-0.147		
Pd	-35.409	n.s.	-23.588	-1.665		
MTsize	227.096	168.869			205.355	160.347
MTshape	n.s.	-16.392			-5.438	-11.675
Constant	-6.397	0.454	7.261	1.592	-27.022	-17.408
Model fit						
AUC	**0.98**	**0.98**	**0.93**	**0.94**	**0.96**	**0.96**
AUC standard error	0.010	0.009	0.019	0.019	0.013	0.017
Kappa	**0.88**	**0.89**	**0.77**	**0.71**	**0.82**	**0.75**
Model fit when applied to live material						
AUC	**0.92**	**0.97**	0.89	**0.91**	**0.92**	**0.94**
AUC standard error	0.042	0.022	0.048	0.046	0.035	0.036
Kappa	**0.76**	**0.79**	0.63	**0.74**	0.65	**0.83**
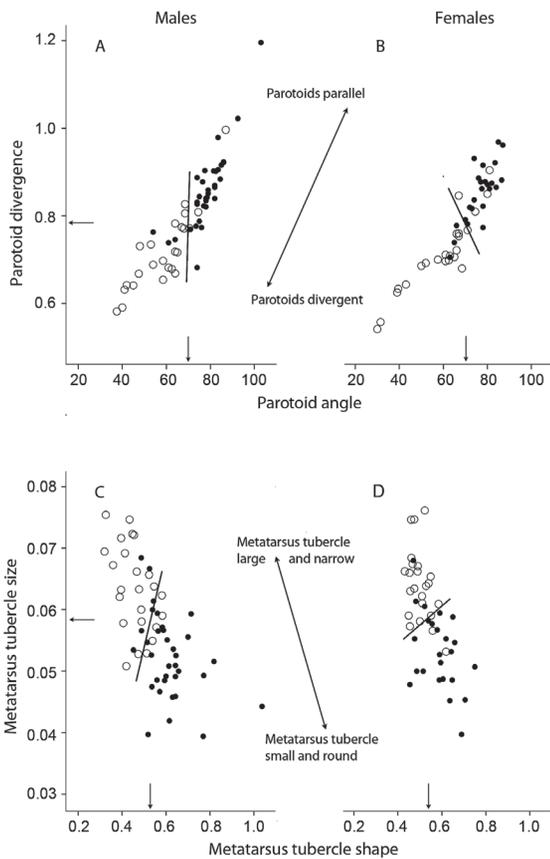
Fig. 4. Bivariate plot of parotoid (top) and metatarsal tubercle (bottom) character sets in *Bufo bufo* (solid dots) and *B. spinosus* (open dots) from Northern France. Males are shown on the left and females on the right. The solid lines show species separation as determined by logistic regression analyses; for formulas and model fit see Table 1. Arrows indicate *B. bufo* versus *B. spinosus* classification criteria (see Discussion).
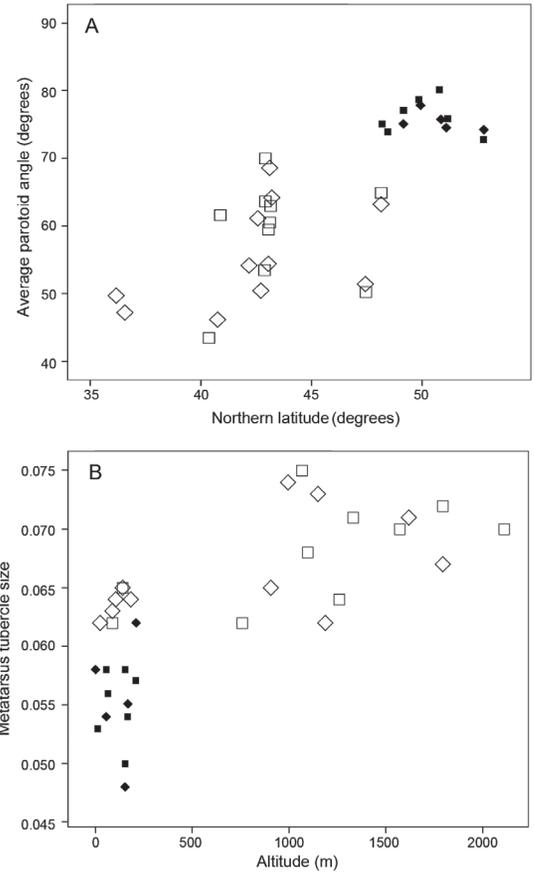

Fig. 5. Variation in A) parotoid angle as a function of degrees northern latitude and B) size of the metatarsus tubercle as a function of altitude observed in male (diamond symbols) and female (square symbols) in *Bufo bufo* (small solid symbols) and *B. spinosus* populations (large open symbols). Shown are averages for populations with a sample size ≥ 5, as in Appendix IV.

≥ 0.93 and kappa ≥ 0.71 (Table 1B). Models for the two data sets were not dissimilar, except that the parameter SUl was not included for the live material and was included for the museum material. When the models derived for live toads were applied to the museum material and *vice versa* model fit was somewhat less good than in the original models, with a drop of 1-6 percentage points in AUC-values.

Seen from the tip of the snout, the parotoids in *B. spinosus* are widely divergent whereas in *B. bufo* they are positioned in parallel or slightly divergent (Fig. 4AB). In *B. bufo* the metatarsal tubercle is small and in *B. spinosus* it is larger (Fig. 2C); in males the tubercle is more round in *B. bufo* and more narrow in *B. spino-*

sus (Fig. 4CD; see Appendix III for absolute values). The analysis of the character Pa in isolation showed that the cut-off point for the species is 70° in males (-0.197*Pa, constant = 13.765; AUC = 0.91 ± 0.045, kappa = 0.76) as well as in females (-0.205*Pa, constant = 14.371; AUC = 0.88 ± 0.051, kappa = 0.66; for an example of a logistic regression equation see the footnote to Table 1).

Intraspecific variation in SUl, Pa, Pd, MTsize and cheek spines is higher in *B. spinosus* than in *B. bufo* from Northwestern Europe. A data summary for field and museum material with N ≥ 5 per population and sex is reported in Appendix IV. Visual inspection of the data against the latitudinal and altitudinal gradi-

ents showed no patterns, other than a tendency in *B. spinosus* from the south of Spain to have widely diverging parotoids (Pa < 50) and for metatarsal tubercles to increase with altitude (Fig. 5).

Twenty-three adult toads for which dorsal images were published (Muratet, 2008; 12 *B. bufo* and 11 *B. spinosus*) were identified using the parotoid characters Pa and Pd with the formulae presented in Table 1. Nineteen toads were classified correctly (83%, AUC = 0.97 ± 0.030; kappa = 0.66). Finally, statistical analysis with Fisher's exact test of the data published by De Lange (1973) on museum preserved toads from Western Europe indicates that *B. spinosus* is more heavily spined than *B. bufo* (males $P < 0.01$, females $P < 0.0001$) and that *B. bufo* females are more heavily spined than males ($P < 0.001$; in *B. spinosus* $P > 0.2$; Appendix VI).

Discussion

Species differentiation, identification and taxonomic status

Lüscher *et al*. (2001) studied 24 toad populations in and around Switzerland at ten allozyme loci and compared these with four Mediterranean populations from France and Italy. Genetic differentiation was minimal, with the exception of two Southern French populations that showed a Nei's genetic distance of ca. 0.19 relative to the remainder. We classify these populations as *B. spinosus* and the others as *B. bufo* (Fig. 1B). The deep genetic differentiation of *B. bufo* and *B. spinosus* was further highlighted by a variety of molecular markers (García-Porta *et al*., 2012; Recuero *et al*., 2012). The available molecular data allow the approximate delimitation of the contact zone of *B. bufo* and *B. spinosus* across France, from Caen at the Atlantic coast, through the upper Rhone valley near Lyon, to the Mediterranean Cote d'Azur (Fig. 1B). A more detailed survey along the mutual range border of *B. bufo* and *B. spinosus* is in progress (Arntzen *et al*., in prep.).

Allele sharing for *B. bufo* and *B. spinosus* was not observed at the *RPL3* locus and species specific mtDNA haplotypes were not found in syntopy, other than at the species contact zone. At *POMC* we recorded a different pattern. Firstly, alleles typical for *B. spinosus* (Arntzen *et al*., 2013) were found in *B. bufo* and not the other way round; this asymmetry is statistically significant (G-test of independence, P<0.001). Secondly, these 'spinosus-alleles' are found not just relatively close to the species contact zone (frequency 30% at

Sorques), but also further away (frequency 25% at Autreppes). An intriguing possibility supported by these observations is that the 'spinosus-alleles' carried by *B. bufo* in Northeastern France constitute 'genetic footprints' (*sensu* Scribner and Avise, 1993), with interspecific gene flow in the direction of the invading species (Currat *et al*., 2008). This would indicate that *B. spinosus* previously had a wider distribution and was subsequently superseded by *B. bufo* over a part of its range, *i.e*., Northeastern France and beyond. If this interpretation is correct, it would be worthwhile to also test for the past presence of *B. spinosus* in the United Kingdom, because we observed one copy of the *POMC* 'spinosus-allele' in Audresselles at the French side of the Chanel and, moreover, one 'spinosus-like' allele at the locality Wymeswold near Leicester in the United Kingdom (Fig. 3; sample BB04 in Recuero *et al*., 2012). However, more data are required before we can rule out the possibility of incomplete lineage sorting to explain allele sharing at *POMC*.

The measurements on live toads in populations at either side of the contact zone confirm that *B. bufo* and *B. spinosus* are morphologically differentiated. With just the panel of 17 scaled morphometric characters it would be more compelling to identify a given individual to the species than to determine its gender. Employing the characters describing the size and the shape of the inner metatarsal tubercle (MTsize and MTshape) and the positioning of the parotoids (Pa and Pd), largely correct species identification is achieved (Table 1). The AUC and kappa values for the various models indicate that species identification based on either the parotoids or the metatarsal tubercle works about equally well (but less well than the data in combination). It is important to note that SUl was not included in the models for this area, indicating that body size does not need to be known for reliable morphometric species identification. Conversely, the models for the museum material all included SUl. The difference can be explained by the wide inverse Bergmannian cline in body size across the *B. bufo* / *B. spinosus* range (Cvetkovic *et al*., 2008; Appendix IV), the effect of which is substantial in the transect spanning Western Europe from 36° - 53° northern latitude, but not noticeable in the sampling area of Northern France that spans less than four degrees. Despite the wide cline, the models derived for live toads in Northern France are highly transferable, *i.e*., they yield a good fit when applied to museum material from across Western Europe (AUC range 0.85-0.95) and *vice versa* (AUC range 0.89-0.97; Table 1).
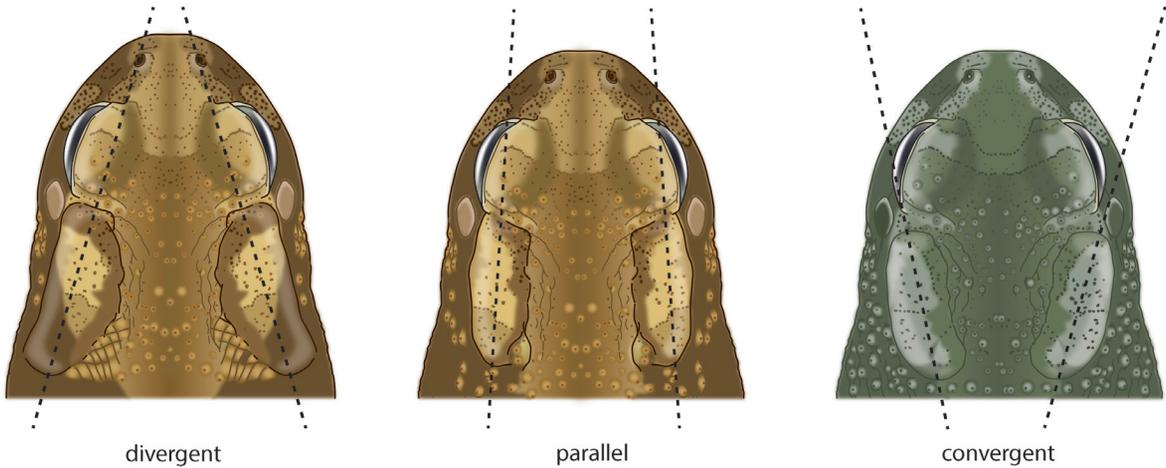
| divergent | parallel | convergent |

Fig. *6*. The positioning of parotoids in toads from Western Europe is, seen in anterior to posterior direction, either divergent (left, *Bufo spinosus*), near-parallel or slightly divergent (middle, *Bufo bufo*) or convergent (right, *Bufo viridis*, shown for comparison; see also Arnold *et al*., 1978). Inter- and intra-specific variation in head shape and parotoid size, shape and positioning of the two former species is illustrated in Appendix V, as observed in Northern France. For morphometric variation over Western Europe see Fig. 5 and Appendix IV.

The parotoids are more widely divergent in *B. spinosus* than in *B. bufo* and the inner metatarsal tubercle is larger in *B. spinosus* than in *B. bufo*. In male toads the tubercle is more rounded in *B. bufo* and narrower in *B. spinosus*. In *B. spinosus* the metatarsal tubercle may be ovoid or pear-shaped, especially in females. Adult *Bufo* toads in Northern France can be identified to the species with the following key:

Parotoids in parallel position or slightly divergent, metatarsal
        tubercle small and round .... *Bufo bufo*
Parotoids divergent, metatarsal tubercle large and narrow ....
.... *Bufo spinosus*

Morphometric criteria to classify live toads from Northern France as *Bufo bufo* and not *B. spinosus* (see also Fig. 4) are:

Character	Character state
Parotoid angle	≥ 70º
Parotoid divergence	> 0.785
Metatarsal tubercle size	< 0.0585
Metatarsus tubercle shape – males	> 0.53
Idem - females	> 0.54

These diagnostic morphological characters have been highlighted in the literature on anuran systematics before. The inner metatarsal tubercle is recognized as a character of taxonomic importance in *e.g.*, European species of green frogs (genus *Pelophylax*). The more terrestrial species inhabiting loose soils *P. lessonae* (Camerano, 1882) has a longer and more prominent metatarsal tubercle than the more aquatic species *P. ridibundus* (Pallas, 1771). Whether there is a parallel with differential ecological preferences of *B. bufo* and *B. spinosus* toads remains to be investigated. To the positioning of the parotoids as 'convergent' as observed in *Bufo viridis* (Laurenti, 1768) and *Bufo calamita* (Laurenti, 1768) or marginally divergent as in *B. bufo*, we add the character state 'divergent' that is observed in *B. spinosus* (Fig. 6). Unfortunately, the taxonomically important characters (MTl, MTw, Pa and Pd) are exactly those that show the highest inter-observer variation in the field. Moreover, in collection material, preservation can affect the shape of the metatarsal tubercle, *e.g.*, when squeezed if there is not enough space in the jars, and parotoids might get flattened and their edges less neat in preserved toads than in live toads. Nevertheless, the criteria for species identification derived from live material in France appear to be applicable to ethanol-preserved material from across Western Europe, as indicated by high model transferability (Table 1). Allometric effects and geographical or clinal variation may come into play, but affect the identification criteria only marginally.

In addition to the morphological and genetic differences between *B. bufo* and *B. spinosus* reported

here, Hemelaar (1988) found a striking difference in life-history between a population of *B. spinosus* from Southern France and populations of *B. bufo* from Switzerland, Germany, Norway and The Netherlands. They grow much faster and mature after having spent ca. 60% longer on growth than *B. bufo* (Hemelaar, 1988), but again, the difference may turn out to be clinal across species instead of abrupt and species-specific, when a wider array of populations is considered (Cvetkovic *et al*., 2008).

Several studies purported to document species differences were based on the assumption that *B. spinosus* is pan-Mediterranean and *B. bufo* a northern species, which we now know is incorrect. For example, bioacoustic differences were documented for toad populations from Hungary and Greece, with statistically significant differences at six out of seven call parameters (Schneider and Sinsch, 2004; Schneider, 2005). Actually, this suggests the presence of a pronounced geographical variation within *B. bufo*, or perhaps a strong effect of body size (see Cvetkovic *et al*., 2008; Gingras *et al*., 2013). Similarly, a high density of cheek warts observed in Italian *B. bufo* (Lüscher *et al*., 2001) indicates that this character state is not typical for *B. spinosus*. Wilkinson *et al*. (2007) reported that the majority of microsatellite loci developed did not amplify well in *Bufo* from two French localities that fall within the range of *B. spinosus*. With the benefit of hindsight this may be attributed to the fact that the primers for these microsatellites were developed for *B. bufo* from the United Kingdom (Brede *et al*., 2001; Brede and Beebee, 2006) and do not amplify well in another species (see also van de Vliet *et al*., 2012).

On account of the deep genetic differentiation, the absence of unequivocal evidence for hybridization of *B. bufo* and *B. spinosus* in the area we investigated, the sister-group relationship of *B. spinosus* and the *B. bufo – B. verrucosissimus* clade and the observed morphological differentiation (Arntzen *et al*., 2013; present paper), we conclude that *B. bufo* and *B. spinosus* are best considered separate species. However, considering that all Mediterranean toad populations were until recently considered *Bufo bufo spinosus* (*e.g*., García-Porta *et al*., 2012), we presume that southern *B. bufo* resemble *B. spinosus* in morphology, but data are scarce (*e.g*., De Lange, 1973). Similarly, eight *Bufo bufo* from the Rhodopi Mountains in Southern Bulgaria had parotoid angles in the *B. spinosus* range (JvA unpublished data: range 43°-68° and average 59.8°, cf. Figs 4 and 5), which on the criterion from western Europe would classify them as *B. spinosus*.

Evolutionary patterns and puzzles

Toads in the *B. bufo* species group have no aposematic coloration, no particular odours and they do not bite. They have no elongated ribs with protruding epipleural processes as in the salamander *Pleurodeles waltl* Michahelles, 1830 that function as a concealed weapon, capable of actively piercing through the skin to hurt a predator, even if at the same time hurting itself (Leydig, 1879; Nowak and Brodie, 1978; Heiss *et al*., 2009). *Bufo* toads are poor jumpers and do not rely on escape behaviour to defer predators and also they do not use the 'Unken reflex' (Duellman and Trueb, 1986). Aside from an inconspicuous life style their main defence mechanism is the possession of parotoid glands from which they can expel a venomous secretion. Also they employ bladder emptying and inflate their lung and, in doing so, the belly, to defend themselves.

Inspired by the observation that the cheek warts are often the largest and most strongly keratinized ones on a toad's body, we suggest that these devices, along with large adult size, a wide head with diverging parotoids and the capability of puffing itself up, assist to counter predators such as snakes that swallow their prey entirely and have limited gape-width. Elias and Shapiro (1957) proposed that the presence of spines on warts might discourage predators in *Bufo americanus* (Holbrook, 1836). The particularly well-developed cheek warts with keratinized spines (see specimen MNCN 25647 in Appendix VII) may thus be analogous to the sharp, backward pointing extensions of the quadratum bones ('quadrate hooks', Brodie *et al*., 1984) in the salamander *Echinotriton andersoni* (Boulenger, 1892). This hypothesis implies that predation by snakes is currently underestimated and that more species have toads on their menu than just the two grass snakes known to consume toads [*Natrix natrix* (Linnaeus, 1758) and *N. maura* (Linnaeus, 1758), see García-París *et al*., 2004; Sinsch *et al*., 2009]. To test our scenario geographical variation can be employed as a tool (cf. Durand *et al*., 2012; Hoso and Hori, 2008). The hypothesis to be tested is that a toad's head is wider, body size larger and cheek warts with keratinized spines more prominent in areas with high densities of bufonivorous snakes. Prey choice experiments with snakes and measurements of rates of successful attacks could be measured on toads differing in these features. However, head width also determines mouth width and thereby the maximum size of prey items that can be swallowed as

toads don't chew up their prey into pieces. The largest prey reported for *B. bufo* / *B. spinosus* are worms, leaches (invertebrates) and among vertebrates lizards, geckos, songbirds and mice (Sinsch *et al.*, 2009). The confounding hypothesis that a wide mouth allows the uptake of larger prey could be tested by studying the menu of toads in northern and southern populations. High levels of fluctuating asymmetry (FA) would not be expected from characters under strong natural selection from predators (Bergstrom and Reimchen, 2003), which runs counter to our observation that parotoid size and shape are highly variable, and fails to explain that FA is higher in males than in females. We consider the study of geographic variation in size and shape of the parotoids and metatarsus tubercle, head width and cheek spines a promising line of research. *Bufo spinosus* is a suitable species for this study, on account of the geographic variation observed at these characters (Fig. 5, Appendices IV and VII).

While head shape has been considered of taxonomic importance (Blair, 1972), the lack of congruence with a molecular phylogeny (Pyron and Wiens, 2011) suggests that the character is highly evolvable. The outgroup to the *B. bufo* – *B. verrucosissimus* – *B. spinosus* clade possesses multiple character states (2/0, 2/2 and 2/3 of Inger, 1973), with a wide skull in *B. gargarizans*, a medium wide skull in *B. tibetanus* Zarevsky, 1926 [note that these taxa are closely related and could not be clearly distinguished by genetic studies (Zhan and Fu, 2011)] and a narrow skull in *Bufo raddei* Strauch, 1876 (Ye *et al.*, 1993). Hence, the polarity of character transformation series cannot be determined, supporting the Pyron and Wiens (2011) view. Yet the most parsimonious scenario is that a wide head represents the ancestral condition in the *B. bufo*, *B. spinosus*, *B. verrucosissimus* species group and that a narrow head is a local adaptation in northern *B. bufo*.

Bufo bufo spinosus is traditionally diagnosed as a Mediterranean taxon with large body size, a parchment-like skin and a dense network of well-developed warts with keratinous spines (De Lange, 1973). The large body suggests a high desiccation tolerance due to a lower surface to volume ratio (Schmidt, 1965), the parchment skin may reduce evaporation and the extensive sculpturing of thickened skin warts may assist passive water uptake (Lillywhite and Licht, 1974, Toledo and Jared, 1993). As many of the warts in *Bufo* include histological elements that resemble tactile corpuscles (Elias and Shapiro, 1957) they may play a role as sensory organs, but why then the expression of warts would vary geographically we do not know. It has been proposed adaptations to a dry environment have evolved in *B. spinosus* and Mediterranean *B. bufo* independently (Lüscher *et al.*, 2001; García-Porta *et al.*, 2012). However, as with head width, an alternative scenario is that the reverse conditions of small body size and a thin and smooth skin are local adaptations of northern *B. bufo*.

References

Arnold EN, Burton JA, Ovenden DW. 1978. A Field Guide to the Reptiles and Amphibians of Britain and Europe. London: Collins.

Arntzen JW, Recuero E, Canestrelli D, Martínez-Solano I. 2013. How complex is the *Bufo bufo* species group? *Molecular Phylogenetics and Evolution* 69: 1203-1208.

Bergstrom CA, Reimchen TE. 2003. Asymmetry in structural defenses: insights into selective predation in the wild. *Evolution* 57: 2128-2138.

Beukema W, de Pous P, Donaire-Barroso D, Bogaerts S, García-Porta J, Escoriza D, Arribas OJ, El Mouden EH, Carranza S. 2013. Review of the systematics, distribution, biogeography and natural history of Moroccan amphibians. *Zootaxa* 3661: 1-60.

Blair WF. 1972. Evolution in the genus *Bufo*. Austin: University of Texas Press.

Bogaerts S, Donaire-Barroso D, Pasmans F, Herbert D, Beukema W. 2013. New data on the distribution of *Bufo bufo* in Tunisia. *Herpetology Notes* 6: 203-207.

Brede EG, Rowe G, Trojanowski J, Beebee TJC. 2001. Polymerase chain reaction primers for microsatellite loci in the common toad *Bufo bufo*. *Molecular Ecology Notes* 1: 308-310.

Brede EG, Beebee TJC. 2006. Consistently different levels of genetic variation across the European ranges of two anurans, *Bufo bufo* and *Rana temporaria*. *Herpetological Journal* 16: 265-271.

Brodie ED, Nussbaum RA, DiGiovanni M. 1984. Antipredator adaptations of Asian salamanders (Salamandridae). *Herpetologica* 40: 56-68.

Cohen J. 1960. A coefficient of agreement for nominal scales. *Educational Psychology Measurement* 20: 37-46.

Currat M, Manuel R, Petit RJ, Excoffier L. 2008. The hidden side of invasions: massive introgression by local genes. *Evolution* 62: 1908-1920.

Cvetkovic D, Tomasevic N, Ficetola GF, Crnobrnja-Isailovic J, Miaud C. 2008. Bergmann's rule in amphibians: combining demographic and ecological parameters to explain body size variation among populations in the common toad *Bufo bufo*. *Journal of Zoological Systematics and Evolutionary Research* 47: 171-180.

De Lange L. 1973. A contribution to the intraspecific systematics of *Bufo bufo* (Linnaeus, 1758) (Amphibia). *Beaufortia* 21 (280): 99-116.

Duellman WE, Trueb L. 1986. Biology of amphibians. New York: McGraw Hill.

Durand J, Legrand A, Tort M, Thiney A, Michiewicz RJ, Coulon A, Aubret F. 2012. Effects of geographic isolation on anti-snakes responses in the wall lizard, *Podarcis muralis*. *Amphibia-Reptilia* 33: 199-206.

Elias H, Shapiro J. 1957. Histology of the skin of some toads and frogs. *Novitates of the American Museum of Natural History* 1819: 1-27.

Flot JF. 2010. SeqPHASE: a web tool for interconverting PHASE input/output files and FASTA sequence alignments. *Molecular Ecology Resources* 10: 162-166.

García-París M, Montori A, Herrero P. 2004. Fauna Ibérica. Madrid: Museo Nacional de Ciencias Naturales-Consejo Superior de Investigaciones Científicas.

García-Porta J, Litvinchuk SN, Crochet PA, Romano A, Geniez PH, Lo-Valvo M, Lymberakis P, Carranza S. 2012. Molecular phylogenetics and historical biogeography of the west-palearctic common toads (*Bufo bufo* species complex). *Molecular Phylogenetics and Evolution* 63: 113-130.

Geniez PH, Cheylan M. 2012. Les amphibiens et les reptiles du Languedoc-Rousillon et regions limitrophes. Atlas biogéographique. Paris: Biotope – Muséum national d'Histoire naturelle.

Gingras B, Boeckle M, Herbst CT, Fitch WT. 2013. Call acoustics reflect body size across four clades of anurans. *Journal of Zoology* 289: 143-150.

Heiss E, Natchev N, Salaberger D, Gumpenberger M, Rabanser A, Weisgram J. 2009. Hurt yourself to hurt your enemy: new insights on the function of the bizarre antipredator mechanism in the salamandrid *Pleurodeles waltl*. *Journal of Zoology* 280: 156-162.

Hemelaar A. 1988. Age, growth and other population characteristics of *Bufo bufo* from different latitudes and altitudes. *Journal of Herpetology* 22: 369-388.

Hoso M, Hori M. 2008. Divergent shell shape as an antipredator adaptation in tropical land snails. *American Naturalist* 172: 726-732.

Inger RF. 1973. *Bufo* of Eurasia. Pp. 102-118 in: Blair WF., ed., *Evolution in the genus* Bufo. Austin: University of Texas Press.

Kutrup B, Yilmaz N, Canakci S, Belduz AO, Doglio S. 2006. Intraspecific variation of *Bufo bufo*, based on 16S ribosomal RNA sequences. *Amphibia-Reptilia* 27: 268-273.

Leydig F. 1879. Die Rippenstacheln des *Pleurodeles waltlii*. *Archiv für Naturgeschichte* 45: 211-234.

Lillywhite HB, Licht P. 1974. Movement of water over toad skin: functional role of epidermal sculpturing. *Copeia* 1974: 165-171.

Litvinchuk SN, Mazepa GO, Kami HG, Auer M. 2012. Taxonomic status and distribution of common toads in Iran. *Herpetological Journal* 22: 271-274.

Lüscher B, Grossenbacher K, Scholl A. 2001. Genetic differentiation of the common toad (*Bufo bufo*) in the Swiss Alps. *Amphibia-Reptilia* 22: 141-154.

Muratet J. 2008. Identifier les Amphibiens de France métropolitaine. Guide de terrain. Avignonet-Lauragais: Association ECODIV.

Nowak RT, Brodie ED. 1978. Rib penetration and associated antipredator adaptations in the salamander *Pleurodeles waltl* (Salamandridae). *Copeia* 1978: 424-429.

Palmer AR, Strobeck C. 1986. Fluctuating asymmetry: measurement, analysis, patterns. *Annual Review of Ecology and Systematics* 17: 391-421

Pyron RA, Wiens JJ. 2011. A large-scale phylogeny of Amphibia including over 2800 species, and a revised classification of extant frogs, salamanders, and caecilians. *Molecular Phylogenetics and Evolution* 61: 543-583.

Recuero E, Canestrelli D, Vörös J, Szabó K, Poyarkov NA, Arntzen JW, Crnobrnja-Isailovic J, Kidov AA, Cogălniceanu D, Caputo FP, Nascetti G, Martínez-Solano I. 2012. Multilocus species tree analyses resolve the radiation of the widespread *Bufo bufo* species group (Anura, Bufonidae). *Molecular Phylogenetics and Evolution* 62: 71-86.

Schmid WD. 1965. Some aspects of the water economies of nine species of amphibians. *Ecology* 46: 261-269.

Schneider H. 2005. Bioakustik der Froschlurche. Einheimische und verwandte Arten. Bielefeld: Laurenti-Verlag.

Schneider H, Sinsch U. 2004. Calls and calling behaviour of the common toad, *Bufo b. bufo*, in Hungary and a comparison with the advertisement call of the giant toad, *Bufo b. spinosus*. *Zeitschrift für Feldherpetologie* 11: 187-201.

Scribner KT, Avise JC. 1993. Cytonuclear genetic architecture in mosquitofish populations and the possible roles of introgressive hybridization. *Molecular Ecology* 2: 139-149.

Sinsch U, Schneider H, Tarkhnishvili D. 2009. *Bufo bufo* Superspezies - Erdkröten-Artenkreis - taxon *bufo* (Linnaeus, 1758) - Erdkröte - taxon *gredosicola* L. Müller and Hellmich 1935 - Gredoserdkröte - taxon *spinosus* Daudin, 1803 - Riesenerdkröte - taxon *verrucosissimus* (Pallas, 1811) - Kolchische Erdkröte. Pp. 191-335 in: Grossenbacher K., ed., *Handbuch der Reptilien und Amphibien Europas, 5/II. Froschlurche (Anura) II (Hylidae, Bufonidae)*. Wiebelsheim: Aula-Verlag.

Sokal RR, Rohlf FJ. 1981. Biometry. Second edition. San Francisco: Freeman and Co.

SPSS. 2013. Statistical Package for the Social Sciences. Chicago: SPSS Inc.

Stephens M, Smith N, Donnelly P. 2001. A new statistical method for haplotype reconstruction from population data. *American Journal of Human Genetics* 68: 978-989.

Swofford DL. 2001. PAUP 4.0b: Phylogenetic Analysis Using Parsimony. Sunderland: Sinauer Associates.

Toledo, RC, Jared C. 1993. Cutaneous adaptations to water balance in amphibians. *Comparative Biochemistry and Physiology, part A* 105: 593-608.

Vliet MS van de, Beebee TJC, Diekmann OE. 2012. Genetic evidence for a distinct *Pelodytes* lineage in southwest Portugal: implications for the use of pre-developed microsatellite markers. *Conservation Genetics* 13: 605-611.

Wilkinson JW, Beebee TJC, Griffiths RA. 2007. Conservation genetics of an island toad: *Bufo bufo* in Jersey. *Herpetological Journal* 17: 192-198.

Ye C, Fei L, Hu S. 1993. Rare and economic amphibians of China. Chengdu: Sichuan Publishing House of Science and Technology. [in Chinese]

Zhan AB, Fu JZ. 2011. Past and present: Phylogeography of the *Bufo gargarizans* species complex inferred from multi-loci allele sequence and frequency data. *Molecular Phylogenetics and Evolution* 61: 136-148.

APPENDICES

Appendix I

Material studied from the collections of the Naturalis Biodiversity Center, Leiden (The Netherlands), the National Museum of Natural History, Paris (France) and the National Museum of Natural Sciences, Madrid (Spain). Coordinates latitude and longitude are in square brackets. Altitudes are in m above sea level (a.s.l.) and approximated with Google Earth. ♂ = male and ♀ =female. Toads from localities a-c, 1-3, 5 and 13 are identified as *Bufo bufo* and all others as *B. spinosus*. For completeness sake we provide the coordinates and altitudes of localities a-e (Fig. 1) as follows: a) Audresselles [50.82134, 1.60194, 10 m.a.s.l.]. b) Autreppes [49.91492, 3.84678, 152 m.a.s.l.]. c) Sorques [48.34485, 2.77790, 65 m.a.s.l.]. d) Jublains [48.23955, -0.55190, 140 m.a.s.l.]. e) Gizeux [47.37608, 0.26945, 88 m.a.s.l.].

Naturalis Biodiversity Center, Leiden, the Netherlands: 1) Charnwood, Colony Reservoir, Coalville, United Kingdom [52.733, -1.313, 208 m.a.s.l.] RenA.ZMA_9291/1-18 ♂♂, RenA.ZMA_9291/19-37 ♀♀. 2) Maastricht [50.85, 5.69, 58 m.a.s.l.] RenA.RMNH_9598/1-3 ♂♂, RenA.RMNH_9598/4-5 ♀♀, RenA.RMNH_9598/6-7 ♂♂, RenA.RMNH_8813/1-6 ♂♂, RenA.RMNH_8813/7-11 ♀♀, RenA.RMNH_9308/1 ♂, RenA.RMNH_9308/2-7 ♀♀. 3) Landgoed Heuven, Rheden, [52.01, 6.03, 13 m.a.s.l.] RenA.RMNH_8143/1-3 ♂♂ RenA.RMNH_8143/4-5 ♀♀.

Muséum national d'Histoire naturelle, Paris, France: 4a) Ariège, Lac de Bethmale [42.860, 1.085, 1065 m.a.s.l.] 1971.0337 ♂. 4b) Ariège, Moulis Labo CNRS [42.950, 1.083, 440 m.a.s.l.] 1971.0338 ♂. 5) Aube, Foret d'Orient [48.31, 4.41, 155 m.a.s.l.] 1988.5659 ♂, 1988.5660 ♂, 1988.5661 ♂, 1988.5662 ♂, 1988.5663 ♂, 1988.5664 ♂, 1988.5665 ♂, 1988.5666 ♂, 1988.5667 ♂. 6) Landes [44.25, 1.00, 64 m.a.s.l.] 1988.6699 ♀. 7) Midi-Pyrénées, Bagnères de Bigorre [43.067, 0.150, 566 m.a.s.l.] 1973.0046 ♀. 8) Midi-Pyrénées, Lac de Bordères [42.861, 0.460, 1785 m.a.s.l.] 1973.0047 ♀. 9) Puerto de Leitariegos, Spain [42.995, -6.412, 1260 m.a.s.l.] 1994.7851 ♂, 1994.7852 ♂, 1994.7853 ♂, 1994.7854 ♂, 1994.7855 ♂. 10) Puy du Dome, Lac de la Cossière [45.67, 3.00, 776 m.a.s.l.] 1988.7763 ♂. 11) Pyrénées Atlantique, Etang du plateau d'Iraty, 6,8 km à l'Ouest du col Bagargui [43.046, -1.074, 1067 m.a.s.l.] 1984.2291 ♂, 1984.2292 ♂, 1984.2293 ♂, 1984.2294 ♂, 1984.2295 ♀, 1984.2296 ♀, 1984.2297 ♂. 12) Rio Dinha, Portugal [40.517, -8.067, 260 m.a.s.l.] 1970.1174

♂, 1970.1175 ♂. 13) Val d'Oise, Carnelle, Lac Bleu [49.120, 2.319, 169 m.a.s.l.] 1988.7544 ♂, 1988.7682 ♀, 1988.7683 ♀, 1988.7685 ♀, 1988.7694 ♀, 1988.7697 ♀, 1988.7699 ♂, 1988.7701 ♂, 1988.7703 ♂, 1988.7706 ♂, 1988.7707 ♀, 1988.7708 ♂, 1988.7710 ♀ and 1988.7711 ♂.

Museo Nacional de Ciencias Naturales, Madrid, Spain: 14) Laguna del Barco, Puerto Castilla, Ávila [40.23, -5.60, 1789 m.a.s.l.] 25331 ♂ and 25332 ♀. 15) San Pedro del Valle (=Xestoso), Rebordelo / Monfero, A Coruña [43.01, -9.17, 105 m.a.s.l.] 25626 ♀, 25627 ♀, 25628 ♀, 25629 ♀, 30480 ♂, 30481 ♀, 42155 ♀. 16) Peña Gorbea, Murguía, Álava [42.96, -2.82, 1332 m.a.s.l.] 25709 ♂, 25710 ♂, 25711 ♂, 25712 ♀, 25713 ♂, 25714 ♂, 25715 ♂ and 25716 ♂. 17) Tanes, Campo de Caso, Asturias [43.18, -5.34, 517 m.a.s.l.] 25497 ♂, 25498 ♂, 25499 ♀, 25500 ♂, 25501 ♀, 25503 ♂ and 25504 ♀. 18a) 13,9 km east of Facinas, Los Barrios, Cádiz [36.19, -5.49, 25 m.a.s.l.] 11132 ♀. 18b) 12,9-23,3 km east of Facinas, Los Barrios, Cádiz [36.19, -5.49, 25 m.a.s.l.] 11133 ♀, 11134 ♂, 11135 ♀, 11136 ♀, 11137 ♂, 11138 ♀ and 11139 ♀. 18c) Los Barrios, Cádiz [36.19, -5.49, 25 m.a.s.l.] 11155 ♀ and 11157 ♀. 18d) Tarifa-Los Barrios, Cádiz [36.19, -5.49, 25 m.a.s.l.] 11152 ♀, 11154 ♀ and 11156 ♀. 19) Alcalá de los Gazules, Cádiz [36.46, -5.72, 185 m.a.s.l.] 11141 ♀, 11142 ♀, 11143 ♀, 11144 ♀, 11145 ♀ and 11147 ♀. 20a) Tarifa, Cádiz [36.01, -5.60, 50 m.a.s.l.] 11151 ♀. 20b) Facinas, Tarifa, Cádiz [36.02, -5.60, 50 m.a.s.l.] 25085 ♀. 21a) Barcenilla, Ruente, Cantabria [43.26, -4.27, 222 m.a.s.l.] 16824 ♀. 21b) Ucieda, Ruente, Cantabria [43.26, -4.27, 198 m.a.s.l.] 25196 ♂. 21c) Río Saja (Ucieda), Ruente, Cantabria [43.26, -4.27, 184 m.a.s.l.] 41483 ♂, 41484 ♀ and 41485 ♀. 22a) Arroyo de la Fuenfría, Puerto de La Fuenfría, Madrid [40.78, -4.05, 1794 m.a.s.l.] 2800 ♂ and 2801 ♂. 22b) Las Dehesas, Cercedilla, Madrid [40.78, -4.05, 1794 m.a.s.l.] 25517 ♀, 25518 ♂, 25519 ♀, 25520 ♂, 25521 ♂, 25522 ♂, 25523 ♂, 25524 ♂, 25525 ♀, 25526 ♂, 25527 ♀, 25528 ♂, 25529 ♂, 25530 ♂, 25531 ♂, 25532 ♂, 25533 ♂, 25534 ♂, 25535 ♂, 25536 ♂, 25537 ♂ and 25538 ♂. 22c) Puerto de La Fuenfría, Madrid [40.78, -4.05, 1794 m.a.s.l.] 25539 ♀. 23a) Cinco Lagunas, Sierra de Gredos, Ávila [40.25, -5.27, 2111 m.a.s.l.] 2729 ♀. 23b) Circo de Gredos, Ávila [40.25, -5.27, 1945 m.a.s.l.] 2782 ♂, 2783 ♂ and 2784 ♂. 23c) Laguna Grande de Gredos, Ávila [40.25, -5.27, 1945 m.a.s.l.] 1852 ♀, 2773 ♀ and 16825 ♀. 23d) Prado de las Pozas, Hoyos del Espino, Ávila [40.25, -5.27, 1931 m.a.s.l.] 30482 ♂, 30483 ♂ and 30484 ♂. 24a) Los Baños de

Benasque, Huesca [42.60, 0.52, 1150 m.a.s.l.] 2740 ♀, 2742 ♀, 2743 ♀, 2744 ♂ and 2745 ♀. 24b) Benasque, Huesca [42.60, 0.52, 1150 m.a.s.l.] 25130 ♀. 25) Ibón de Piedrafita, Huesca [42.70, -0.36, 1618 m.a.s.l.] 9528 ♀, 9529 ♀, 9530 ♀, 9532 ♀, 9533 ♀, 9534 ♀, 9535 ♀, 9536 ♂, 9537 ♂, 9538 ♂ and 25141 ♀. 26) El Pueyo de Jaca, Panticosa, Huesca [42.72, -0.28, 1097 m.a.s.l.] 9926 ♂, 9927 ♀, 9928 ♀, 9929 ♂, 9930 ♂, 9931 ♂, 9932 ♂, 9933 ♀ and 9934 ♂. 27) Selva de Oza, Hecho, Huesca [42.74, -0.75, 823 m.a.s.l.] 9941 ♀ and 9948 ♀. 28) Monasterio de Valvanera, Anguiano, La Rioja [42.23, -2.87, 995 m.a.s.l.] 25690 ♀, 25691 ♀, 25692 ♀, 30605 ♀, 30606 ♂, 30607 ♀, 30608 ♂, 30609 ♀, 30610 ♂, 30611 ♀, 30612 ♂, 30613 ♀, 30614 ♀, 30615 ♀ and 30616 ♀. 29) Nacimiento del Río Oja, Sierra de la Demanda, Ezcaray, La Rioja [42.33, -3.01, 1430 m.a.s.l.] 25695 ♂. 30) Puerto de Vegarada, Valdelugueros, León [43.03, -5.48, 1572 m.a.s.l.] 13003 ♂, 13004 ♀, 13005 ♀, 13006 ♂, 13007 ♂, 13008 ♀, 13009 ♂ and 13010 ♂. 31) La Milla del Río, Carrizo, León [42.58, -5.83, 875 m.a.s.l.] 13174 ♂. 32) La Uña, Acebedo, León [43.03, -5.13, 1189 m.a.s.l.] 25367 ♂, 25368 ♀, 25369 ♀, 25370 ♂, 25371♀, 25373 ♀ and 25375 ♀. 33a) A Pobra de Burón, Fonsagrada, Lugo [43.13, -7.06, 907 m.a.s.l.] 25636 ♀, 25637 ♀, 25638 ♀, 25639 ♀, 25640 ♀, 25641 ♀, 25642 ♀, 25643 ♀, 25644 ♀, 25645 ♀, 25647 ♀, 25648 ♂, 25649 ♀, 25651 ♀, 25652 ♀, 25653 ♀ and 25654 ♀. 33b) Pedrafitelas, Fonsagrada, Lugo [43.13, -7.06, 907 m.a.s.l.] 25646 ♀, 26205 ♀ and 42154 ♀. 34) Frigiliana, Málaga [36.79, -3.90, 324 m.a.s.l.] 25110 ♀, 25111 ♀, 25112 ♂, 25114 ♂, 25115 ♂, 25116 ♂, 25117 ♀ and 25118 ♀. 35) Tleta-Ketama, Morocco [34.88, -4.62, 1300 m.a.s.l.] 645 ♀. 36) Imlil, Morocco [31.13, -7.92, 1911 m.a.s.l.] 2749 ♀, 2750 ♀ and 2751 ♂. 37) Río Urtxurria, Bosque de Irati, Ochagavia, Navarra [42.91, -1.09, 760 m.a.s.l.] 2760 ♂, 2761 ♂, 2762 ♂, 2763 ♂ and 2765 ♂. 38) Elizondo (Baztán), Navarra [43.14, -1.52, 202 m.a.s.l.] 25580 ♀, 25584 ♀, 25589 ♀ and 25590 ♀. 39) Sierra do Gerês, Pitoes, Portugal [41.73, -8.16, 382 m.a.s.l.] 25075 ♀. 40a) Porto Covo - S. do Cacem, Portugal [several localities] 24584 ♀, 24585 ♀, 24586 ♀, 24587 ♂, 24588 ♂ and 24589 ♂. 40b) Porto Covo, Portugal [37.85, -8.79, 25 m.a.s.l.] 16612 ♂. 40c) Castillo de la Isla do Pessegueiro, Porto Covo, Portugal [37.83, -8.80, 0 m.a.s.l.] 24582 ♀.

Appendix II

Restriction profile of the *Bufo* cytochrome b sequence after treatment with the endonuclease *Bcu*I. *Bufo bufo* has two recognition sites for this enzyme whereas
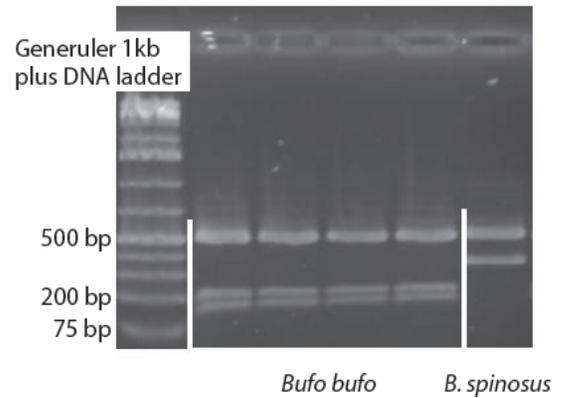
B. spinosus has one, resulting in three and two size fragments, respectively.

Appendix III

Bivariate plot of untransformed measurements on the length and width of the metatarsal tubercle in male (top) and female toads (bottom), taken on live material in the field, Northern France (left) and in museum collections from across Western Europe (right). Solid dots represent *Bufo bufo* and open dots represent *B. spinosus*. Data are summarized by convex polygons. Note the wide spread in the preserved material that, however, does not seem to compromise species identification.
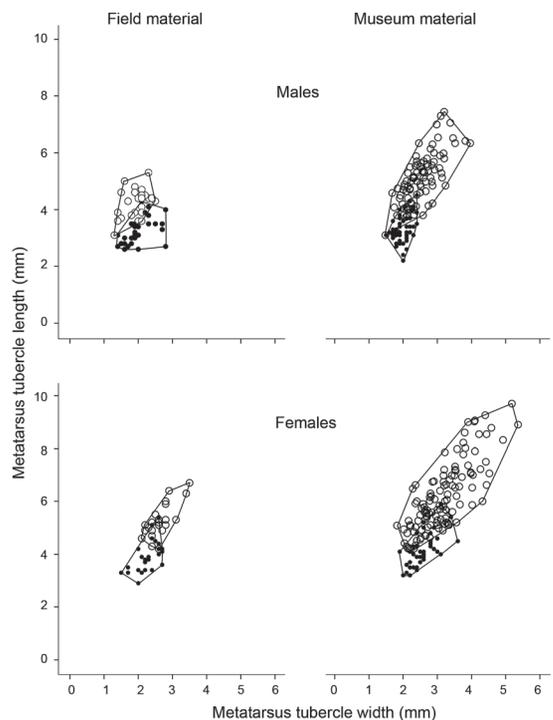
Appendix IV

Summary of inter- and intra-specific morphological variation (average, standard deviation (SD), 95% confidence interval of the average (CI95 low and high) and range (min-max)) in *Bufo bufo* and *B. spinosus* populations for which sample size N ≥ 5. Top panel - males, middle panel - females, bottom panel – cheek spines for males and females (preserved material only). For population localities see Fig. 1 (a-e, live material) and Appendix I (1-40, preserved material). Toads from localities a-c, 1-3, 5 and 13 are identified as *Bufo bufo* and all others as *B. spinosus*.

Males

Character	Population	N	Average	SD	CI95low	CI95high	Min	Max
Snout Urostyle length (mm)								
	a	11	60.7	4.41	57.77	63.69	55.0	71.0
	b	15	61.8	4.02	59.57	64.03	57.0	70.0
	c	8	68.3	5.85	63.36	73.14	56.0	76.0
	d	13	63.6	4.23	61.06	66.17	58.0	72.0
	e	11	70.5	4.03	67.75	73.17	65.0	77.5
	1	18	53.5	4.11	51.46	55.54	44.0	63.0
	2	12	62.0	3.16	59.99	64.01	57.0	66.0
	5	9	57.8	2.58	55.85	59.82	54.0	61.0
	9	5	78.9	3.95	74.01	83.83	74.0	84.0
	11	5	69.0	8.03	59.05	78.99	60.0	76.0
	13	8	59.8	2.88	57.40	62.22	57.0	64.0
	16	7	59.6	5.26	54.71	64.43	54.0	70.0
	22	20	70.5	3.99	68.63	72.37	65.0	78.0
	23	6	79.3	5.32	73.75	84.91	73.0	89.0
	26	6	84.2	10.59	73.05	95.28	70.0	97.0
	30	5	66.4	5.13	60.03	72.77	60.0	73.0
	37	5	60.4	2.88	56.82	63.98	57.0	64.0
Parotoid angle (degrees)								
	a	11	80.3	4.25	77.42	83.13	73.5	86.0
	b	15	78.5	10.01	72.99	84.08	54.0	103.0
	c	8	75.0	10.00	66.64	83.36	61.0	92.5
	d	13	65.2	10.59	58.83	71.63	40.0	87.0
	e	11	51.0	10.04	44.30	57.79	37.5	68.5
	1	18	72.8	6.36	69.62	75.94	61.0	83.0
	2	12	75.3	7.78	70.31	80.20	66.0	92.0
	5	9	74.2	6.08	69.55	78.89	63.0	85.0
	9	5	59.6	4.22	54.36	64.84	54.0	65.0
	11	5	63.5	10.09	50.98	76.03	51.0	76.0
	13	8	77.1	8.65	69.90	84.35	64.5	89.5
	16	7	63.7	6.40	57.80	69.63	55.0	70.5
	22	20	61.9	7.40	58.39	65.31	43.5	76.0
	23	6	43.7	9.02	34.20	53.13	29.0	56.5
	26	6	53.8	7.99	45.45	62.22	40.0	61.0
	30	5	60.5	5.71	53.41	67.59	54.5	66.5
	37	5	70.0	9.69	57.97	82.03	62.5	85.0
Parotoid divergence (Pda (mm)/Pdp (mm))								
	a	11	0.85	0.048	0.820	0.884	0.77	0.92
	b	15	0.88	0.114	0.814	0.940	0.68	1.20
	c	8	0.83	0.094	0.755	0.911	0.74	1.02
	d	13	0.74	0.100	0.682	0.803	0.59	1.00
	e	11	0.69	0.072	0.644	0.740	0.58	0.83
	1	18	0.83	0.066	0.801	0.867	0.69	0.93
	2	12	0.90	0.060	0.858	0.934	0.83	1.01

5	9	0.83	0.037	0.798	0.856	0.78	0.89
9	5	0.76	0.039	0.711	0.809	0.70	0.80
11	5	0.82	0.022	0.792	0.847	0.80	0.85
13	8	0.89	0.059	0.837	0.936	0.80	0.96
16	7	0.82	0.047	0.773	0.859	0.75	0.86
22	20	0.75	0.067	0.720	0.783	0.60	0.89
23	6	0.65	0.042	0.609	0.697	0.60	0.72
26	6	0.68	0.076	0.598	0.759	0.59	0.76
30	5	0.77	0.055	0.701	0.837	0.70	0.84
37	5	0.80	0.054	0.738	0.872	0.74	0.88

Metatarsal tubercle size (MTl (mm) / SUl (mm))

a	11	0.053	0.0067	0.0489	0.0579	0.044	0.067
b	15	0.050	0.0074	0.0455	0.0538	0.039	0.068
c	8	0.056	0.0032	0.0532	0.0585	0.050	0.060
d	13	0.065	0.0073	0.0604	0.0693	0.051	0.075
e	11	0.062	0.0069	0.0571	0.0663	0.053	0.075
1	18	0.057	0.0068	0.0538	0.0605	0.046	0.069
2	12	0.058	0.0072	0.0538	0.0629	0.048	0.070
5	9	0.058	0.0060	0.0534	0.0626	0.051	0.070
9	5	0.064	0.0061	0.0565	0.0716	0.060	0.074
11	5	0.075	0.0144	0.0576	0.0933	0.064	0.100
13	8	0.054	0.0055	0.0490	0.0583	0.049	0.065
16	7	0.071	0.0080	0.0637	0.0785	0.056	0.080
22	20	0.072	0.0117	0.0665	0.0775	0.054	0.095
23	6	0.070	0.0049	0.0653	0.0755	0.062	0.077
26	6	0.068	0.0026	0.0654	0.0709	0.065	0.072
30	5	0.070	0.0056	0.0631	0.0770	0.062	0.076
37	5	0.062	0.0059	0.0549	0.0695	0.054	0.070

Metatarsal tubercle shape (MTw (mm) / (MTl (mm))

a	11	0.67	0.160	0.560	0.775	0.51	1.04
b	15	0.59	0.076	0.545	0.629	0.45	0.77
c	8	0.59	0.069	0.536	0.651	0.49	0.70
d	13	0.44	0.092	0.388	0.498	0.32	0.58
e	11	0.48	0.048	0.444	0.508	0.40	0.55
1	18	0.67	0.103	0.617	0.720	0.50	0.91
2	12	0.60	0.063	0.564	0.644	0.51	0.69
5	9	0.52	0.031	0.496	0.544	0.47	0.57
9	5	0.46	0.056	0.389	0.529	0.40	0.54
11	5	0.47	0.052	0.406	0.535	0.42	0.53
13	8	0.61	0.070	0.551	0.669	0.51	0.71
16	7	0.46	0.051	0.414	0.509	0.39	0.55
22	20	0.49	0.068	0.461	0.525	0.39	0.68
23	6	0.52	0.097	0.416	0.619	0.41	0.67
26	6	0.50	0.077	0.423	0.585	0.42	0.62
30	5	0.47	0.044	0.419	0.527	0.43	0.53
37	5	0.54	0.049	0.479	0.601	0.48	0.61

Females

Character	Population	N	Average	SD	CI95low	CI95high	Min	Max
Snout Urostyle length (mm)								
	a	11	73.4	4.39	70.42	76.31	67.0	79.0
	b	10	71.8	3.46	69.33	74.27	66.0	78.0
	d	16	83.8	8.75	79.15	88.48	67.0	98.0
	e	7	80.4	6.86	74.01	86.70	73.0	89.5
	1	19	65.4	7.16	61.97	68.87	52.0	78.0
	2	13	75.0	4.88	72.05	77.95	69.0	83.0
	13	6	73.5	5.72	67.51	79.52	67.0	80.0
	15	6	76.3	8.04	67.89	84.77	65.0	87.0
	18	11	102.4	25.45	85.26	119.46	69.0	150.0
	19	6	101.7	11.76	89.33	114.01	89.0	117.0
	22	5	93.6	13.61	76.70	110.50	79.0	114.0
	24	5	91.4	16.07	71.44	111.36	80.0	119.0
	25	8	102.8	7.03	96.88	108.62	95.0	115.0
	28	11	78.9	11.78	71.00	86.82	67.0	99.0
	32	5	83.0	3.16	79.07	86.93	80.0	88.0
	33	19	84.2	6.82	80.92	87.50	74.0	96.0
Parotoid angle (degrees)								
	a	11	75.7	8.32	70.14	81.32	63.0	87.0
	b	10	78.1	4.46	74.91	81.29	71.0	86.5
	d	16	62.7	13.78	55.38	70.06	31.5	81.0
	e	7	51.4	13.22	39.13	63.59	30.0	66.0
	1	19	74.4	10.31	69.43	79.36	52.5	92.0
	2	13	74.5	9.07	68.98	79.94	55.0	91.0
	13	6	75.0	8.03	66.58	83.42	63.0	85.0
	15	6	68.7	11.95	56.12	81.21	50.5	83.0
	18	11	49.9	13.16	41.02	58.71	30.5	65.5
	19	6	47.4	5.48	41.67	53.17	40.5	57.0
	22	5	46.2	18.23	23.57	68.83	20.5	69.5
	24	5	61.0	14.71	42.73	79.27	36.0	75.0
	25	8	50.4	6.51	45.00	55.88	41.0	59.5
	28	11	54.1	14.17	44.57	63.61	23.5	82.5
	32	5	54.3	8.03	44.33	64.27	41.5	62.0
	33	19	63.7	8.17	59.80	67.67	45.0	75.5
Parotoid divergence (Pda (mm)/Pdp (mm))								
	a	11	0.84	0.089	0.784	0.904	0.71	0.97
	b	10	0.86	0.038	0.833	0.888	0.78	0.92
	d	16	0.73	0.089	0.686	0.781	0.56	0.90
	e	7	0.67	0.070	0.608	0.737	0.54	0.76
	1	19	0.88	0.071	0.843	0.911	0.76	0.99
	2	13	0.86	0.064	0.819	0.897	0.73	0.96
	13	6	0.86	0.069	0.792	0.936	0.78	0.94
	15	6	0.84	0.063	0.778	0.911	0.73	0.90
	18	11	0.68	0.098	0.615	0.746	0.51	0.80
	19	6	0.68	0.053	0.624	0.735	0.58	0.73
	22	5	0.63	0.107	0.501	0.767	0.50	0.77
	24	5	0.72	0.041	0.670	0.771	0.67	0.77
	25	8	0.71	0.050	0.670	0.754	0.62	0.78
	28	11	0.74	0.074	0.687	0.787	0.60	0.85
	32	5	0.74	0.052	0.674	0.802	0.68	0.81
	33	19	0.81	0.079	0.774	0.850	0.69	0.95

Metatarsal tubercle size (MTl (mm) / SUl (mm))

a	11	0.058	0.0045	0.0546	0.0606	0.051	0.068
b	10	0.048	0.0036	0.0451	0.0502	0.040	0.053
d	16	0.065	0.0066	0.0610	0.0681	0.053	0.076
e	7	0.063	0.0037	0.0596	0.0665	0.058	0.067
1	19	0.062	0.0075	0.0586	0.0658	0.052	0.081
2	13	0.054	0.0061	0.0504	0.0577	0.044	0.069
13	6	0.055	0.0044	0.0503	0.0595	0.051	0.061
15	6	0.064	0.0076	0.0565	0.0724	0.058	0.078
18	11	0.062	0.0053	0.0582	0.0653	0.051	0.069
19	6	0.064	0.0077	0.0560	0.0721	0.054	0.075
22	5	0.067	0.0035	0.0624	0.0711	0.061	0.071
24	5	0.073	0.0078	0.0632	0.0826	0.068	0.087
25	8	0.071	0.0091	0.0636	0.0788	0.060	0.089
28	11	0.074	0.0044	0.0711	0.0770	0.070	0.084
32	5	0.062	0.0059	0.0551	0.0697	0.056	0.068
33	19	0.065	0.0076	0.0616	0.0690	0.052	0.083

Metatarsal tubercle shape (MTw (mm) / (MTl (mm))

a	11	0.58	0.082	0.526	0.637	0.47	0.75
b	10	0.59	0.084	0.532	0.652	0.45	0.71
d	16	0.51	0.050	0.488	0.541	0.45	0.62
e	7	0.47	0.029	0.445	0.499	0.43	0.51
1	19	0.65	0.059	0.621	0.678	0.50	0.78
2	13	0.63	0.077	0.587	0.680	0.50	0.80
13	6	0.58	0.073	0.498	0.652	0.46	0.66
15	6	0.50	0.084	0.408	0.585	0.36	0.61
18	11	0.56	0.043	0.531	0.589	0.51	0.64
19	6	0.54	0.051	0.485	0.593	0.48	0.63
22	5	0.49	0.056	0.420	0.559	0.40	0.54
24	5	0.48	0.086	0.373	0.586	0.35	0.59
25	8	0.52	0.096	0.440	0.600	0.40	0.67
28	11	0.49	0.065	0.446	0.533	0.41	0.60
32	5	0.61	0.072	0.525	0.703	0.54	0.72
33	19	0.53	0.076	0.494	0.568	0.44	0.68

Cheek spine scores

Sex	Population	N	Average	Sex	Population	N	Average
Males	1	18	1.00	Females	1	19	1.00
	2	12	2.08		2	13	2.23
	3	3	1.67		3	2	2.00
	5	9	1.89		13	6	1.83
	9	5	3.00		15	6	4.17
	11	5	3.00		18	11	3.73
	13	8	1.38		19	6	4.17
	16	7	1.43		22	5	4.00
	22	20	2.55		24	5	3.20
	23	6	2.33		25	6	3.67
	26	5	3.20		28	11	3.45
	30	5	2.00		32	5	2.40
	37	5	2.00		33	19	3.89

Appendix V

Schematic drawings to illustrate variation in head shape and parotoid position and shape of *Bufo* toads. Parotoids are in grey. Top row are males and bottom row are females. From left to right toads originate from a) Audresselles, b) Autreppes, c) Sorques, d) Jublains and e) Gizeux. Localities a-c have *B. bufo*, d and e have *B. spinosus*. The drawing is purported to illustrate difficulties in measuring 'parotoid divergence' (Pd) because parotoid length may be asymmetric (*e.g.*, male from Sorques, female from Autreppes) or parotoid start and end may be difficult to determine due to interaction with dorsal warts (*e.g.*, male and female from Sorques). Occasionally parotoids may be curved or oblique (illustrated in Arnold *et al*. 1978: 65 and Muratet 2008: 181 female, 187 Fig. 5b) which makes it difficult to measure 'parotoid angle' (Pa). Also note the spines at the cheek in the female from Gizeux.
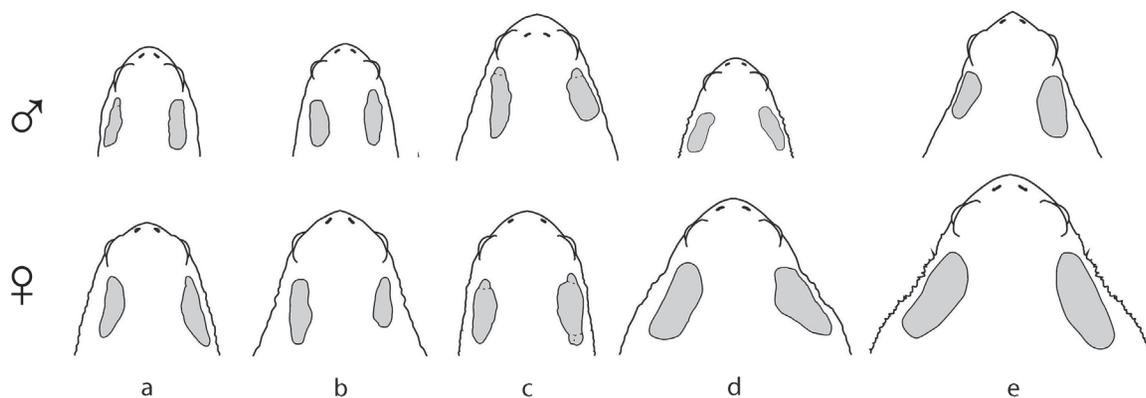
Appendix VI

The degree to which *Bufo bufo* and *B. spinosus* skins have smooth versus spined warts, as recorded by De Lange (1973: Fig. 2). Categories are 'smooth' (De Lange's classes 1 - 3 in which warts are smooth, without keratinized spines), 'slightly spined' (De Lange's class 4 - with keratinized pigmented spine tops) and 'heavily spined' (De Lange's classes 5 and 6 - with fully keratinized single or double spines). Toads from the De Lange's regions I and II are interpreted as *Bufo bufo* (the north of France and northwards) and those from region III as *B. spinosus* (the south of France and southwards). Inspection of the collection of the Naturalis Biodiversity Center identified six specimens from Italy – also in region III - that were excluded from the data set.

Species	*Bufo bufo*		*Bufo spinosus*	
Sex	Males	Females	Males	Females
Skin wart structure				
Smooth	37	50	3	1
Slightly spined	17	70	1	2
Heavily spined	1	15	3	9

Appendix VII

The warts on the cheek are often the biggest ones on a toad's body and frequently furnished with keratinized spines, such as here shown in six adult specimens of *Bufo spinosus*. All toads are females, except for MNCN 25526 and 25522 which are males. Categories discerned in the character 'cheek spines' in lateral view are: 1 - absent (MNCN 25526), 2 – slight (MNCN 30481), 3 – medium (MNCN 25522), 4 – strong (MNCN 11132) and 5 - very strong (MNCN 1852). Photo 6 illustrates an extreme case of category 5 in dorsal view (MNCN 25647).
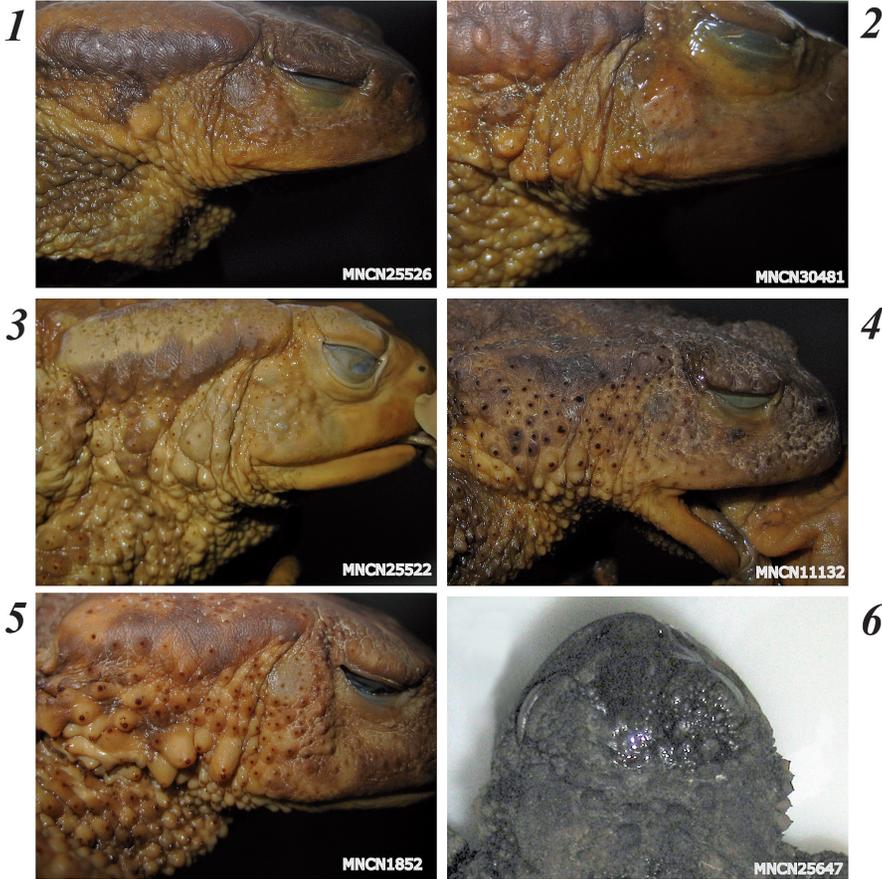
Appendix VIII

Distribution data of species in the *Bufo bufo* species group after Arntzen *et al.* (2013). Documented localities of *Bufo* species in Europe and North Africa, with *Bufo spinosus* in red, *B. bufo* in blue, *B. verrucosissimus* in brown and *B. eichwaldi* in green. Data sources are: Kutrup *et al.* (2006) open round symbols in Italy and Turkey, Recuero *et al.* (2012) solid round symbols, García-Porta *et al.* (2012) square symbols, Litvinchuk *et al.* (2012) green triangle symbols, Beukema *et al.* (2013) and Bogaerts *et al.* (2013) red triangle symbols. The 'S' stands for 28 *B. bufo* populations from in and around Switzerland that were studied by Lüscher *et al.* (2001) while five other of their populations are shown by the '¶' symbol. Records from the present paper are shown by diamond symbols for museum material and open round symbols in France for genetic data; two French localities with *B. bufo* and *B. spinosus* genetic markers in sympatry are indicated by a black cross. The locality Erloy in Northern France where *B. bufo* and *B. spinosus* exclusive alleles of the gene POMC are found in sympatry is shown by the # symbol. For Far-eastern *B. bufo* localities see Recuero *et al.* (2012) and for the range border of the *B. bufo* – *B. spinosus* – *B. verrucosissimus* group across Eurasia see Sinsch *et al.* (2009).